ECS Transactions, 35 (1) 1131-1136 (2011)
10.1149/1.3570094 ©The Electrochemical Society

Chemical Expansion and Frozen-in Oxygen Vacancies in Pr-doped Ceria

Y. Kuru[a,b], S. R. Bishop[a], J. J. Kim[a], B. Yildiz[b], and H. L. Tuller[a]

[a] Department of Materials Science & Engineering, Massachusetts Institute of Technology
77 Massachusetts Avenue, Cambridge, MA 02139, USA
[b] Department of Nuclear Science & Engineering, Massachusetts Institute of Technology
77 Massachusetts Avenue, Cambridge, MA 02139, USA

Doped CeO_2 is a promising candidate for solid oxide fuel cell electrolyte and electrode applications because of its high ionic conductivity and reduction/oxidation behavior at intermediate temperatures. Its electronic and ionic properties and microstructural stability are of particular interest. The present study demonstrates that the large number of oxygen vacancies created in $Pr_xCe_{1-x}O_{2-\delta}$ (PCO) at elevated temperatures can be accommodated at room temperature if cooling is performed in relatively low oxygen partial pressures (i.e. $P(O_2) \sim 10^{-3}$ mbar). We use the temperature dependence of the chemical expansion in reduced PCO as a metric to explore this phenomenon.

Introduction

Both undoped and doped ceria (CeO_2) are of scientific and technological interest. Firstly, it is a model material that helps us to simplify and understand fundamental questions about, for instance, interaction of defects and relationship between residual stresses and defect equilibria since it has a high melting point and a simple fluorite structure (1,2). Secondly, from the application point of view, it has a range of appealing properties such as high oxygen ionic conductivity, large deviations from stoichiometry, mixed ionic electronic conductivity, chemical expansion at reduced oxygen partial pressures, chemical stress and strain effects (1-7). Acceptor doped ceria is regarded as a promising candidate for several applications as solid oxide fuel cell components (8), oxygen sensors (9) and catalysts (10) due to its high ionic conductivity at intermediate temperatures and reduction/oxidation behavior.

In the fuel cell application, CeO_2-based solid electrolytes are in contact with both highly oxidizing (cathode) and reducing conditions (anode). Therefore, it is crucial to know how they will respond (chemically, mechanically and microstructurally) to variations in the operating conditions (i.e. temperature, *T*, and oxygen partial pressure). In this work, we have, as part of a more extensive examination of the electrical, mechanical and defect properties of $Pr_xCe_{1-x}O_{2-\delta}$ (PCO) over a wide range of temperature and $P(O_2)$, studied the chemical expansion, thermal expansion and reduction/oxidation behavior of nanocrystalline $Pr_xCe_{1-x}O_{2-\delta}$ powders and a bulk ceramic, produced from these powders, by *in situ* X-ray diffraction (XRD) between room temperature and 1075°C in air and at low oxygen partial pressures (i.e. $P(O_2) \sim 10^{-3}$ mbar).

Experimental Methods

Nanocrystalline PCO powders were produced by a Pechini-type sol-gel process allowing for the preparation of complex oxides with homogeneous distribution of the constituent metal ions at the molecular level (11,12). Cerium (III) nitrate hexahydrate (99.99%; Sigma Aldrich), praseodymium (III) nitrate hydrate (99.9%; Alfa Aesar), ethylene glycol (99%; Alfa Aesar) and citric acid anhydrous (Fisher Scientific) were used to prepare PCO solid solutions with x=0.1 and 0.2. Aqueous solutions of cerium (III) nitrate and praseodymium (III) nitrate were mixed together by stirring. Afterwards, citric acid and ethylene glycol were added into the solution to form a gel. The mole ratio of citric acid to metal ion was 2:1. The resultant mixtures were stirred at 80 °C until polyesterification between the citric acid and ethylene glycol formed a dry gel. After being dried in an oven at 110°C for 12 h, the powder was ground in a zirconia mortar. Thereafter, they were prefired at 300 and 450°C for 4 h under air. The sample was fully calcined at 700°C for 3 h and milled for 12 h in isopropyl alcohol with zirconia balls as the final step. A PCO ceramic with x=0.1 was prepared by sintering the nanocrystalline powder at 1450°C. The resulting specimen had an average grain size of 2 μm.

The 2θ-ω scans (2θ is the angle between the incident and the diffracted X-ray beams; ω is the angle between the incident beam and the specimen surface) were performed by a PANalytical Expert Pro MPD diffractometer having programmable incident-beam divergence slits and a high-speed high-resolution X'Celerator position-sensitive detector employing Cu Kα radiation. An Anton Paar HTK1200N furnace, capable of heating the specimen from 25 to 1200°C, was mounted to the diffractometer as the sample stage during *in situ* heating experiments. The lattice parameters of the powders were determined by Nelson-Riley extrapolation (i.e. plotting the lattice constant, a, against the Nelson-Riley function and taking the intercept of the line fitted to the data) (13). The crystallite size, D, and the microstrain (i.e. related with the local variations in lattice spacings), ε, were determined by the Williamson-Hall method (14). In this method, differentiation of size and microstrain broadenings is based on the dependence of each broadening type on θ (14). In order to determine the instrumentally broadened profile of the diffractometer as a function of diffraction angle 2θ, 13 *hkl* reflections of a LaB_6 (NIST SRM660) standard powder sample were measured.

The microstructures of the as-prepared and heat-treated $Pr_{0.2}Ce_{0.8}O_{2-\delta}$ powders were characterized in a JEOL 2010 FEG Analytical Electron Microscope operating at an accelerating voltage of 200 kV.

Results and Discussion

The PCO powders used in this study were found to be single phase and cubic fluorite within the detection limits of XRD, both in the as-deposited state as well as after following different temperature and oxygen partial pressure anneals. Figure 1 shows a representative XRD plot of a PCO specimen with x=0.2 measured in vacuum (i.e. $P(O_2) \sim 10^{-3}$ mbar). All 13 peaks can be indexed by the fluorite phase. The D value calculated from Figure 1 by the Williamson-Hall method is about 15 nm, matching well with the average grain size value obtained from transmission electron microscopy investigations.

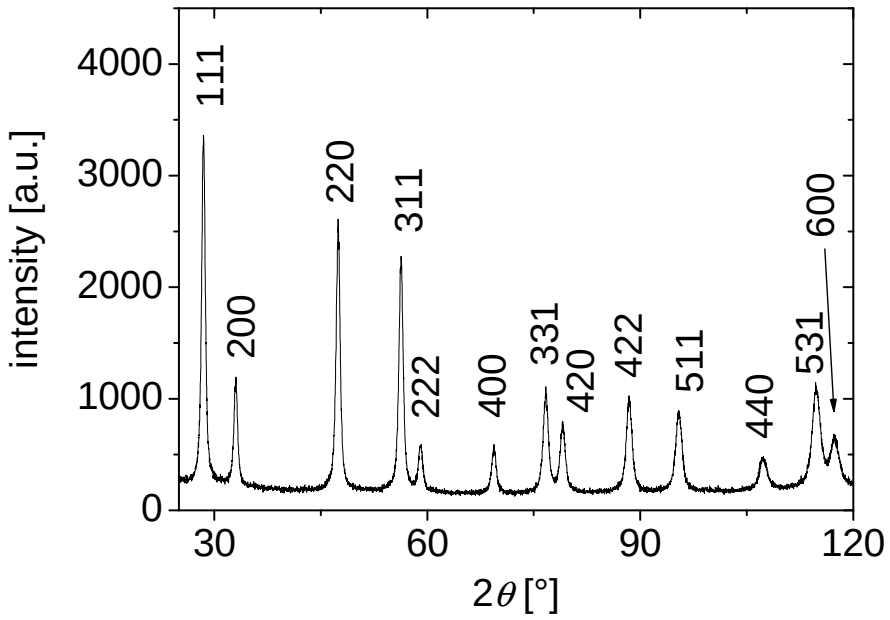

Figure 1. A representative XRD pattern of the PCO powder with x=0.2 in vacuum. All peaks are indexed according to the cubic fluorite phase.

The expansion of the PCO lattice with increasing temperature, *T*, stems from two sources, namely: (i) thermal expansion due to asymmetry of the potential energy versus interatomic distance curve and (ii) chemical expansion due to reduction of Pr^{4+} and/or Ce^{4+} cations to their respective +3 valance states. The latter is accompanied by oxygen loss from the lattice via reactions [1] and/or [2], written according to the Kröger-Vink notation (6,15).

$$2Pr_{Ce}^{x} + 4O_{O}^{x} \leftrightarrow V_{O}^{\bullet\bullet} + \frac{1}{2}O_2 + 2Pr_{Ce}^{'} + 3O_{O}^{x} \quad [1]$$

$$2Ce_{Ce}^{x} + 4O_{O}^{x} \leftrightarrow V_{O}^{\bullet\bullet} + \frac{1}{2}O_2 + 2Ce_{Ce}^{'} + 3O_{O}^{x} \quad [2]$$

The variation of a_0 with *T* for PCO powder with x=0.2 was measured between 25 and 1075°C in vacuum and is presented in Figure 2. During heating to 200°C, a_0 increases with *T*, as expected from its coefficient of thermal expansion. Thereafter, the increase of a_0 as a function of *T* becomes unexpectedly large, presumably, because of the onset of Pr reduction. This is followed by a near plateau in a_0 between ~ 300 and 450°C and then a resumption in the increase with a_0 with increasing T. The *plateau* region may reflect some partial reoxidation or presence of a defect association/dissociation reaction upon heating over this narrow temperature region. Upon cooling from 1075°C, the measured a_0 values (i.e. full circles) coincide well with the ones measured during heating (i.e. full squares) until reaching 675°C. The heating and cooling curves deviate from each other below this temperature presumably because the nanocrystalline PCO powder is not readily re-oxidizing upon cooling at a rate of 1 °C/min in relatively low oxygen pressure.

While the chemical expansion coefficient, $\alpha_{\text{Chem}} = \frac{1}{a} \cdot \frac{\partial a}{\partial \delta}$, is an important parameter in terms of structural stability, we use it here as a metric for estimating the oxygen

vacancy concentration in the lattice. The α_{Chem} value recently obtained in our study is 0.09 corresponding to a δ value of 0.06 (16). This indicates that the majority of the oxygen deficiency created at elevated temperatures, during the reduction of Pr^{4+}, is trapped at ambient temperature kinetically.

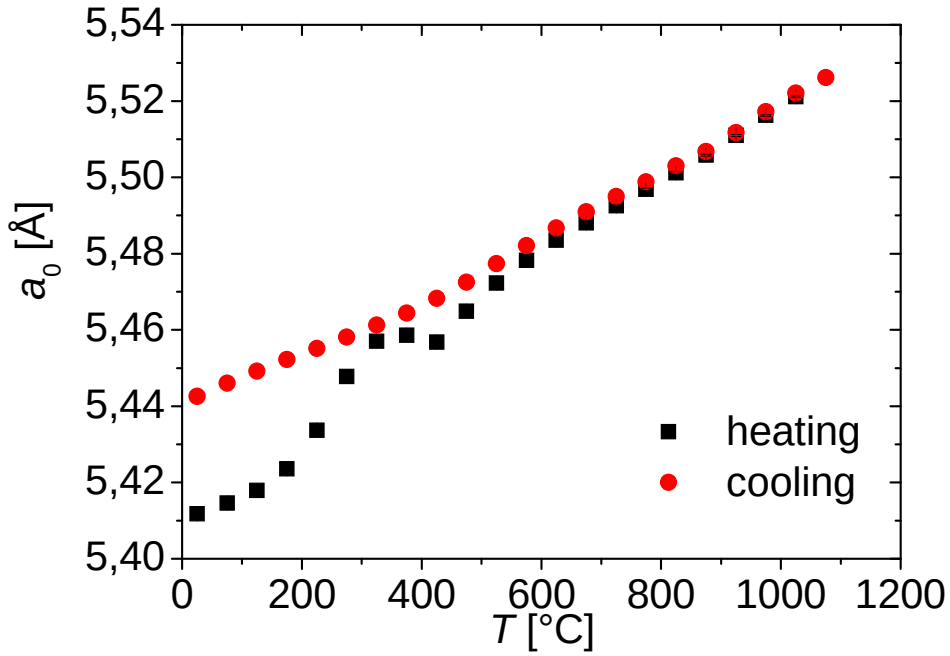

Figure 2. The lattice parameter, a_0, versus temperature, T, for PCO powder with x=0.2 during both heating and cooling. The measurements were performed in vacuum and the error bars are on the order of the symbol size.

A similar experiment is carried out using a bulk PCO specimen with x=0.1 (see Experimental); it is heated from 25 to 1075°C (i.e. black circles in Figure 3) in vacuum (i.e. $P(O_2) \sim 10^{-3}$ mbar). Only thermal expansion is observed between 25 and 600°C. Then, chemical expansion becomes active between 600 and 1000 °C, saturating at around 1000°C since most of the Pr^{4+} cations appears to be reduced to the +3 state by that point. In this case, δ is approximately 0.05 according to reaction [1] indicating that 2.5% of the oxygen sites are vacant. We note that these vacancies can be trapped in the PCO structure at room temperature as in the case of nanocrystalline PCO with x=0.2 (cf. Figure 2 and Figure 3) if cooling is performed in vacuum (i.e. solid black line in Figure 3). Following cooling to room temperature in vacuum, the heating chamber is vented to atmospheric pressure and the specimen is heated again (red circles in Figure 3). PCO retains a lattice expansion commensurate with extra trapped vacancies in the structure below 300°C, and begins to re-oxidize at above 200°C. Similar features in Figure 2 and Figure 3 demonstrate that oxygen vacancies can be trapped at room temperature in both nanocrystalline PCO powder and bulk microcrystalline PCO. On the other hand the kinetics associated with the reduction process upon heating are much accelerated, as expected, in the nanocrystalline PCO as illustrated in Figure 2. Kinetic stabilization of oxygen vacancies may have interesting consequences on the low temperature electrical properties, a feature currently under investigation.

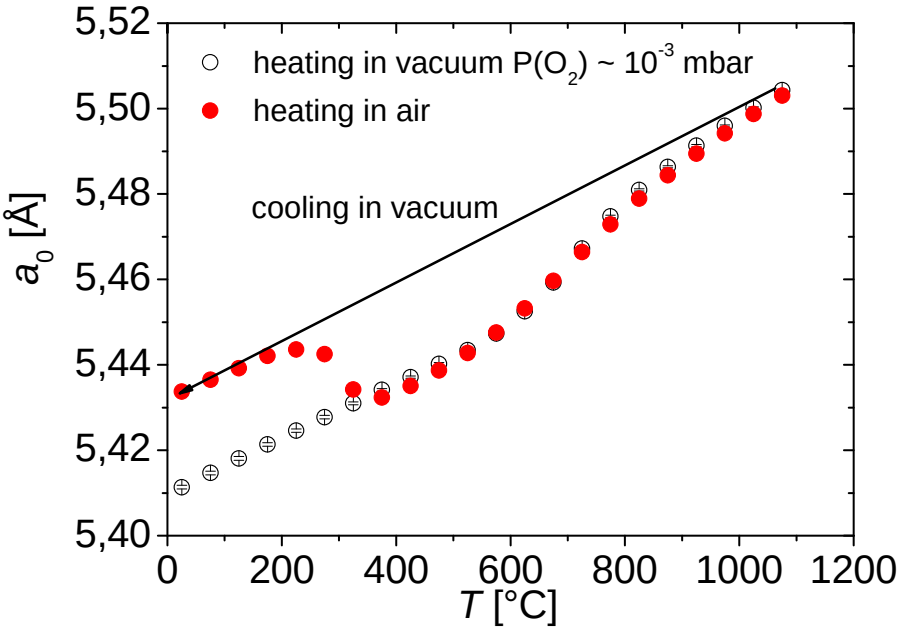

Figure 3. The lattice parameter, a_0, versus temperature, T, for coarse-grained bulk PCO with x=0.1 upon heating to 1075 °C (i.e. black circles) and cooling down to ambient temperature (i.e. black solid line) in vacuum. The red circles denote a_0 versus T of the same specimen after venting the heating chamber at room temperature and reheating. The error bars are of the order of the symbol size.

Conclusions

The oxygen deficiency reached at elevated temperatures can be retained at room temperature if the reduced PCO is cooled under relatively low oxygen partial pressures (i.e. $P(O_2) \sim 10^{-3}$ mbar). This property does not depend on grain size since similar results are obtained for both coarse-grained and nanocrystalline specimens. The extra oxygen vacancies can be accommodated in the structure to above ~ 200°C, which may have interesting consequences on the low temperature electrical properties of $Pr_xCe_{1-x}O_{2-\delta}$.

Acknowledgments

This research is being funded by the MIT Energy Initiative Seed Fund Program and by Basic Energy Sciences, Department of Energy under award DE SC0002633. J. J. Kim thanks The Kwanjeong Educational Foundation and The MIT Energy Initiative for partial fellowship support. The X-ray measurements were performed at MIT's Center of Materials Science and Engineering, an NSF MRSEC funded facility.

References

1. A. Kossoy, Y. Feldman, R. Korobko, E. Wachtel, I. Lubomirsky and J. Maier, *Adv. Funct. Mater.*, **19**, 634 (2009).
2. R. Smith, *Electrochem. Solid-State Lett.*, **10**, A1 (2007).

3. A. Kossoy, Y. Feldman, E. Wachtel, K. Gartsman, I. Lubomirsky, J. Fleig and J. Maier, *Phys. Chem. Chem. Phys.*, **8**, 1111 (2006).
4. H. L. Tuller, *Solid State Ionics*, **131**, 143 (2000).
5. A. Atkinson, *Solid State Ionics*, **95**, 249 (1997).
6. S. R. Bishop, D. Chen, Y. Kuru, J.-J. Kim, T. S. Stefanik and H. L. Tuller, *ECS Trans.*, accepted for publication.
7. S. R. Bishop, T. S. Stefanik and H. L. Tuller, to be published.
8. A. Kossoy, Y. Feldman, E. Wachtel, I. Lubomirsky and J. Maier, *Adv. Funct. Mater.*, **17**, 2393 (2007).
9. P. G. Bruce, *Solid State Electrochemistry*, Cambridge University Press, Cambridge, 1995.
10. A. Trovarelli, *Catal. Rev. Sci. Eng.*, **38**, 439 (1996).
11. M. Kakihana and M. Yoshimura, *Bull. Chem. Soc. Jpn.*, **72**, 1427 (1999).
12. X. Liu and J. Lin, *Solid State Sci.*, **11**, 2030 (2009).
13. B. D. Cullity and S. R. Stock, *Elements of X-ray Diffraction* Prentice-Hall, Englewood Cliffs, 2001.
14. G. K. Williamson and W. H. Hall, *Acta Metall.*, **1**, 22 (1953).
15. Y. -M. Chiang, D. Birnie III and W. D. Kingery, *Physical Ceramics: Principles for Ceramic Science and Engineering*, John Wiley & Sons, Inc., New York, 1997.
16. S. R. Bishop, Y. Kuru and H. L. Tuller, to be published.